Water Research X 14 (2022) 100129

Contents lists available at ScienceDirect

Water Research X

journal homepage: www.sciencedirect.com/journal/water-research-x

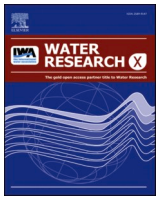

A comprehensive kinetic model for phenol oxidation in seven advanced oxidation processes and considering the effects of halides and carbonate

Kuan Huang, Huichun Zhang *

Department of Civil and Environmental Engineering, Case Western Reserve University, Cleveland, OH 44106, USA

ARTICLE INFO

Keywords:
H_2O_2
Kinetic modeling
Peroxydisulfate
Peroxymonosulfate
Sensitivity analysis
UV irradiation

ABSTRACT

As one of the most powerful approaches to mechanistically understanding complex chemical reactions and performing simulations or predictions, kinetic modeling has been widely used to investigate advanced oxidation processes (AOPs). However, most of the available models are built based on limited systems or reaction mechanisms so they cannot be readily extended to other systems or reaction conditions. To overcome such limitations, this study developed a comprehensive model on phenol oxidation using over 540 reactions, covering the most common reaction mechanisms in nine AOPs—four peroxymonosulfate (PMS), four peroxydisulfate (PDS), and one H_2O_2 systems—and considering product formation and the effects of co-existing anions (chloride, bromide, and carbonate). Existing models in the literature were first gathered and then revised by correcting inaccurately used reactions and adding other necessary reactions. Extensive model tuning and validation were next conducted by fitting the model against experimental data from both this study and the literature. The effects of anions were found to follow PDS/CuO > H_2O_2/UV > other PDS or PMS systems. Halogenated organic byproducts were mainly observed in the PMS systems in the presence of halides. Most of the 543 reactions were found to be important based on the sensitivity analysis, with some anions-involved reactions being among the most important, which explained why these anions substantially altered some of the reaction systems. With this comprehensive model, a deep understanding and reliable prediction can be made for the oxidation of phenol (and likely other phenolic compounds) in systems containing one or more of the above AOPs.

1. Introduction

Advanced oxidation processes (AOPs) are among the most important water treatment technologies for organic contaminant removal. They often rely on the activation of oxidants, such as peroxymonosulfate (PMS), peroxydisulfate (PDS), and H_2O_2, by either energy inputs or catalysts to induce the formation of reactive oxygen species (ROSs), including sulfate ($SO_4^{\bullet-}$) and hydroxyl ($^{\bullet}OH$) radicals (Lee et al., 2020a; Wang and Wang, 2018). Recent studies also reported the involvement of singlet oxygen ($^1O_2$) or direct electron transfer processes in some of the AOP systems (Duan et al., 2018b; Huang and Zhang, 2019). Utilizing the unique long-distance electron transfer property of the prepared catalyst, recent studies developed a "Galvanic oxidation process" that achieved contaminant oxidation even when PMS and the contaminant were physically separated from each other (Huang and Zhang, 2019; 2020a). The reaction mechanisms in AOPs are usually complex as the reactions between ROSs and organic contaminants generate many intermediates/products, which can further react with the ROSs. The persistence and risks of these intermediates/products may also vary significantly. Moreover, various impact factors, such as the coexisting anions, exist in real water treatment scenarios, as mentioned later. These anions can sometimes significantly alter the reaction mechanisms and impact the contaminant removal efficiency, oxidant utilization efficiency, and product formation. Therefore, advanced experimental, computational, and modeling approaches are needed to investigate these AOPs.

Kinetic modeling is a powerful approach to gaining mechanistic understandings of these systems and can help formulate strategies for improving the treatment efficiency. Extensive modeling studies have been reported for many AOPs, such as H_2O_2/UV, PDS/UV, chlorine/UV, and chloramine/UV (Chuang et al., 2017; Crittenden et al., 1999; Grebel et al., 2010; Yang et al., 2014; 2016). Some best examples include 180 reactions for an H_2O_2/UV system (Grebel et al., 2010), 188 reactions for H_2O_2/UV and PDS/UV systems (Yang et al., 2014), 140 reactions for H_2O_2/UV and PDS/UV systems (Zhang et al., 2015), and 203 reactions for HOCl/UV, H_2O_2/UV, and O_3/UV systems (Bulman et al., 2019). A

* Corresponding author.
E-mail address: hjz13@case.edu (H. Zhang).

https://doi.org/10.1016/j.wroa.2021.100129
Received 8 September 2021; Received in revised form 1 December 2021; Accepted 18 December 2021
Available online 21 December 2021

number of studies have also considered intermediate transformation in their kinetic models (Duesterberg and Waite, 2006; C.K. 2007; Guo et al., 2014b; Kang et al., 2002; Li et al., 2004; K. 2007; Luo et al., 2021; Mora et al., 2011; Qian et al., 2016; Zhao et al., 2021; Zhou et al., 2018). For example, Li et al. performed a kinetic modeling of trichloroethene degradation considering four intermediates and 67 reactions in one system (H_2O_2/UV) (K. Li et al., 2007). Duesterberg and Waite modeled the oxidation of p-hydroxybenzoic acid in the H_2O_2/Fe system with 49 reactions and considering one intermediate (3,4-dihydroxybenzoic acid) (C.K. Duesterberg and Waite, 2007). However, most of these models were built on limited numbers of systems under well-defined experimental conditions, so they cannot be readily applied to other systems or conditions. New models therefore need to be developed every time for new systems. This is time consuming and labor intensive. Furthermore, a large portion of the reaction rate constants in some studies were set as the fitting parameters (e.g., 12 out of 67 (K. Li et al., 2007), or 13 out of 101 (Qian et al., 2016)). The number of these fitting parameters is generally much larger than that of the datasets (experimental conditions) used for the model fitting, which may cause over-parameterization. This is similar to solving multivariable equations, where a unique solution is only possible when the number of the equations is equal to or larger than that of the variables. If such a condition is not met, the true values of the variables (or, in this case, the unknown rate constants) cannot be obtained. Therefore, perfect fittings under the studied conditions can be easily obtained but poor fittings are usually expected for other conditions because the fitted rate constants are likely not accurate. To overcome both the applicability limitation and overparameterization issues, we need to build a robust and comprehensive model considering multiple systems and experimental conditions.

The performance of AOPs is also known to be affected by halides (including Cl^- and Br^-) or carbonate (collectively referred to as "the anions" hereafter), often through generating different reactive species. For example, Grebel et al. demonstrated that carbonate significantly decreased the phenol degradation rate in an H_2O_2/UV system because the reaction of $^{\bullet}OH$ with carbonate forms less reactive carbonate radicals ($CO_3^{\bullet-}$). Such an effect is much stronger than that of Cl^- but weaker than that of Br^- (Grebel et al., 2010). In PMS-based systems, halides have reportedly accelerated the contaminant removal because the reactions of PMS with halides form non-radical reactive halogen species (RHSs) (e.g., HOX, X_2, X = Cl or Br) (Fang et al., 2016; Luo et al., 2019; Wang et al., 2017). These non-radical RHSs can sometimes be very abundant compared to the original ROSs and result in significantly faster contaminant oxidation, although they may also lead to inhibited mineralization and formation of toxic halogenated byproducts (Fang et al., 2016; Luo et al., 2019; Wang et al., 2017). Given the ubiquitous presence of these anions in the aquatic environment, it is important to systematically evaluate their impacts on the performance of different AOPs under various conditions. However, current studies considering anions only focused on very limited numbers of oxidants, activation approaches, and reaction mechanisms in each model. The inclusion of additional oxidants/activation approaches may require many more reactions which have not been previously considered.

To address the above limitations, a comprehensive model needs to be developed for a large number of systems covering multiple known oxidants and activation mechanisms. It can also be easily applied to, for instance, compare the performance of different systems side by side or simulate scaled-up water treatment systems under various conditions without having to conduct experimental tests. When hybrid systems are employed in some water treatment scenarios where multiple reactants and/or activation mechanisms are involved (e.g., PDS and H_2O_2 coupled with UV, catalyst, and heat (Monteagudo et al., 2015)), this comprehensive model would be very powerful to describe the systems and provide mechanistic insights.

In this work, four PMS, four PDS, and one H_2O_2 systems were first experimentally evaluated for phenol oxidation in both the absence and presence of the anions. Then a comprehensive kinetic model was developed for 7 AOPs considering different oxidants, activation approaches, reaction mechanisms, and other impact factors. The HOX/UV systems were also included in the model because they existed under some conditions (e.g., the PMS/UV system containing Cl^- and Br^- resulting in HOCl/UV and HOBr/UV systems). The intermediate transformation was also modeled. Phenol was selected as the model compound because it is widely used in industries and is toxic to aquatic life (Olmez-Hanci and Arslan-Alaton, 2013). Although phenol can be relatively easily oxidized by AOPs, it is the most basic phenolic compound and shares significant similarity with many other contaminants. Using phenol would be, therefore, helpful to develop a model that can be easily adopted for a wide range of contaminants. Further, recent advances in tools for oxidation pathway generation (Guo et al., 2014a, 2014b) and reaction rate constant prediction (e.g., quantitative structure-activity relationship (QSAR) models (Zhong et al., 2020a, 2020b)) can also greatly expand the application of this model to other organics. Extensive model tuning and validation were then carried out by fitting the model against the experimental data from both this study and the literature. Detailed balancing was performed to fix the reaction loop illegality issue, and the model sensitivity analysis was conducted to evaluate the importance of each reaction. With the developed model, the effect of anions on the reaction mechanisms and the importance of different ROSs responsible for phenol degradation and product formation, were finally evaluated.

2. Materials and methods

Details in chemicals and materials used in this study can be found in the Supplementary Material (SM) Text S1. The AOP systems were selected to include most of the known reaction mechanisms associated with the oxidants PMS, PDS, and H_2O_2; activation approaches; and responsible ROSs. A total of four PMS, four PDS, and one H_2O_2 systems were investigated (details in Text S2). Detailed experimental procedures and analytical methods can be found in Text S3 and Table S1, including the UV intensity and pathlength determination, catalyst preparation, experimental setup, and the quantification of PMS, PDS, H_2O_2, phenol, and the degradation products.

2.1. Kinetic modeling

The model development consisted of four stages, i.e., initial development, improvement, tuning, and validation. We first conducted an extensive literature review and compiled all the major reactions that may occur in the studied systems using the search engine Google Scholar with the following keywords: advanced oxidation processes, AOPs, kinetic modeling, peroxymonosulfate, PMS, peroxydisulfate, PDS, H_2O_2, phenol oxidation pathways, sulfate radicals, hydroxyl radicals, UV chlorine, UV bromine, and radical reaction rate constant. The resulted records (more than 5000) were screened by checking whether they contained useful contents, such as the pathways and reaction rate constants of the oxidant activation reactions, ROS transformation, and phenol transformation reactions and product formation. This resulted in more than 100 kinetic modeling studies and various books and databases (details in Table S2). Most of the reaction rate constants were obtained from the literature. In case different values were found for a reaction rate constant (reactions listed in Table S3), the average was used if two were retrieved ($n = 2$), or median if more than two were retrieved ($n > 2$). For reactions with unknown rate constants, if the reactions were between organics and radicals, they were estimated based on the linear correlations between the natural log of the second-order rate constant k ($ln\ k$) and the reduction potentials of the radicals (Grebel et al., 2010; Pavitt et al., 2017; Zagal et al., 2019), details in Fig. S1 and Table S4. Others were assumed based on similar reactions and reactants. A total of 40 were estimated or assumed (Table S2). As a result, only eight rate constants were unknown and, therefore, set as the fitting

parameters when fitting the model against the experimental data. Most of these eight rate constants were for initiation reactions, for example, the activation of PMS by catalysts (Eqs. 1 and 3 in Table S5)). For reactions that were inaccurately applied in the literature, revisions were also made (details in Section 3.3). The whole model was built using the computer program Kintecus 6.8 (Ianni, 2019). To include the effects of ionic strength and temperature on the reaction rate constants, the Davies Equation and the Van't Hoff rules, respectively, were applied (details in Text S4).

For the UV-based systems, the photolysis rate of the oxidants for the formation of radicals may change considerably throughout the reaction due to the changing chemical composition. More details about how to dynamically calculate the photolysis rate of a given system in Kintecus can be found in Text S5 and Table S6.

Details of stages 1–4 of the model development can be found in Text S6.

2.2. Detailed balancing using DETBAL, model overparameterization control, and model sensitivity analysis

A variety of techniques were employed in this study during the model development, including detailed balancing using DETBAL (Fig. S2), model overparameterization control, and model sensitivity analysis. More details about these techniques can be found in Texts S7-S9.

3. Results and discussion

3.1. Performance of the nine AOP systems

The phenol degradation rates and oxidant utilization efficiencies were compared in the absence and presence of the anions (including Cl^-, Br^- and HCO_3^-), as shown in Fig. 1. In the three UV systems without the anions, PDS showed the highest phenol degradation rate followed by H_2O_2 and then PMS, while this order changed to PDS > PMS > H_2O_2 in the presence of the anions. The orders of the oxidant utilization efficiencies were H_2O_2 > PDS > PMS and PMS > PDS > H_2O_2 under the UV condition with and without the anions, respectively. These different orders were mainly due to the different photoproperties of these oxidants and the reaction rate constants of phenol/intermediates with different ROSs. Additional discussion of the observed performances can be found in Text S10.

3.2. Initial model development (stage 1)

This stage of the model development mainly involved the initiation reactions (Table S5) and the transformation of ROSs. Overall, the fittings were poor for most of the systems (with R^2 in the ranges of 0.94 – 0.96 and 0.16 – 0.97 for phenol and the oxidant, respectively, as shown in Table S7). For example, for the PMS/UV and PDS/UV systems, the phenol degradation rates were underestimated at the beginning but overestimated at the end of the reactions (Fig. S3). This is probably because some important reactions and intermediate transformations were not yet considered. As the reaction continues, intermediates may compete with the parent compound for the consumption of ROSs to decrease the phenol degradation rate. Therefore, considering more

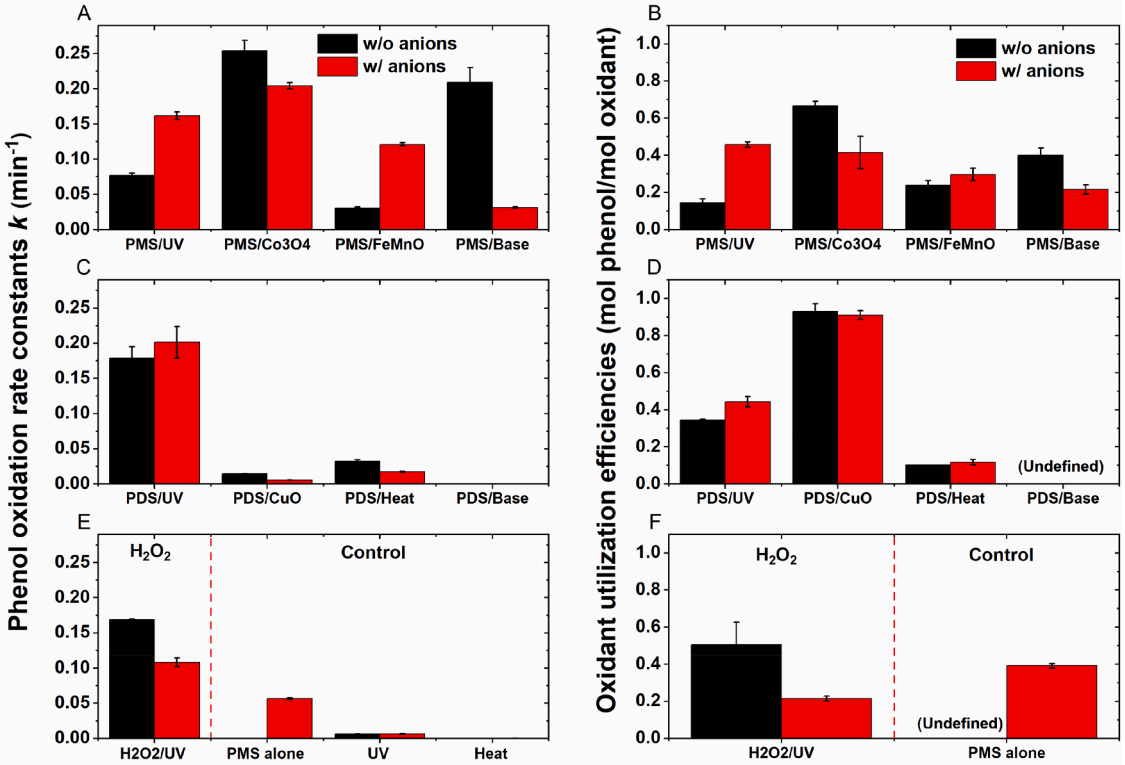

Fig. 1. Left: Pseudo-first order phenol degradation rate constants in (A) PMS, (C) PDS, (E) H_2O_2 and the corresponding control systems. Right: oxidant utilization efficiencies of (B) PMS, (D) PDS, (F) H_2O_2 and the corresponding control systems. No bars on the left panel indicate no appreciable phenol transformation detected. The oxidant utilization efficiencies are "undefined" in some systems (D and F) because the oxidant consumption (denominator) is zero. Experimental conditions: $[oxidant]_0 = 1$ mM, $[phenol]_0 = 50$ μM, pH = 7 with 20 mM of borate buffer for all but the base systems. The activation conditions included UV at 254 nm (for UV systems), heat at 70 °C (for PDS/heat system), base at pH 10 with 20 mM of borate buffer (for base systems), or catalyst at 0.1 g/L (for catalyst systems). "w/ anions" indicated $[Cl^-]_0 = 141$ mM, $[Br^-]_0 = 0.05$ mM, and $[HCO_3^-]_0 = 11.5$ mM. Error bars represent the data range of experimental replicates ($n \geq 2$).

reactions as well as the formation of intermediates/products may significantly improve the model. Nevertheless, at the current stage, we also observed that, according to the primary ROS transformation pathways in the presence of halides (Scheme S1), some of the species such as $Cl_2^{\bullet-}$, $Br_2^{\bullet-}$, $Cl^{\bullet}$, and $HO_2^{\bullet}$ served as important intermediates for the transformation of other species. Some of them such as $Cl_2^{\bullet-}$ and $Br_2^{\bullet-}$ were indeed later found to be important in the contaminant oxidation (Section 3.6).

3.3. Model improvement (stage 2)

In the process of model development, we observed that some reactions had been inaccurately used in some of the previous modeling studies (details in Text S11). For example, O_2 was often treated as the product in the $^{\bullet}OH + HO_2^{\bullet}/O_2^{\bullet-}$ type of reactions (Reactions 100–103, Table S2) (Cheng et al., 2018; Crittenden et al., 1999; Grebel et al., 2010; Yang et al., 2014). However, recent studies have performed convincing experiments, such as the enhancing and quenching tests on a chemiluminescence system, electron spin resonance, and chemical trapping by mass spectrometry, to demonstrate the formation of $^1O_2$ rather than O_2 (Li et al., 2015; Lin and Liu, 2008; Liu et al., 2006; Qi et al., 2016; Zhou et al., 2013). The $^{\bullet}OH + HO_2^{\bullet}/O_2^{\bullet-}$ type of reactions is the primary step in the formation of $^1O_2$ in base-activated PMS (Duan et al., 2018b; Qi et al., 2016). The reactions of radical RHSs with $HO_2^{\bullet}$ or $O_2^{\bullet-}$, including Reactions 56, 57, 78, 79, 119, 137, and 138 in Table S2, should also form $^1O_2$ instead of O_2 because these RHSs can be easily converted from and to $^{\bullet}OH$. In addition, the oxygen as a product in the reactions of H_2O_2 with HOX/X_2 has been reported to be all at the excited state ($^1O_2$), as shown in Reactions 108, 111, 112, 123, 128, 129, 130, and 134 in Table S2 (Held et al., 1978; Khan and Kasha, 1970; Piatt and O'brien, 1979). Therefore, although many modeling studies adopted O_2 rather than $^1O_2$ (Bulman et al., 2019; Cheng et al., 2018; Grebel et al., 2010; Yang et al., 2014; Zhang et al., 2015), we adopted $^1O_2$ as the product here.

Studies have also frequently neglected the important roles of $S_2O_8^{\bullet-}$ and $ClO^{\bullet}$. As they have been proven to be strong oxidants and can effectively oxidize a wide range of organic contaminants (Alfassi et al., 1988; Bulman et al., 2019; Duan et al., 2018a; Kong et al., 2018; Wu et al., 2016), they were included in the model. More details can be found in Text S11.

Upon the incorporation of the above reactions, the improved model was fitted against the experimental data, as shown in Figs. 2A-G. By making the four unavailable rate constants (Reactions 1, 3, 5, and 6 in Table S2) as the fitting parameters, we were able to obtain good fittings for all the seven systems with and without the anions (14 systems in total, with the R^2 in the ranges of 0.98 – 0.999 and 0.62 – 0.99 for phenol and the oxidant, respectively, as shown in Table S7). This suggested that the model can describe the systems well. The correction and inclusion of the above reactions in the model significantly improved the model performance. This improvement can also be explained by the important contributions of $S_2O_8^{\bullet-}$ and $ClO^{\bullet}$ to phenol oxidation, as examined in Section 3.6. The sensitivity analysis in Section 3.8 further confirmed that a number of the above reactions indeed ranked high in the overall importance (Table S8). When differences were found for some rate constants in the literature, they generally differ by less than one order of magnitude. The use of the mean ($n = 2$) or median ($n > 2$) for modeling did not differ significantly compared to using other values (data not shown). Another indication of the good model performance is that the

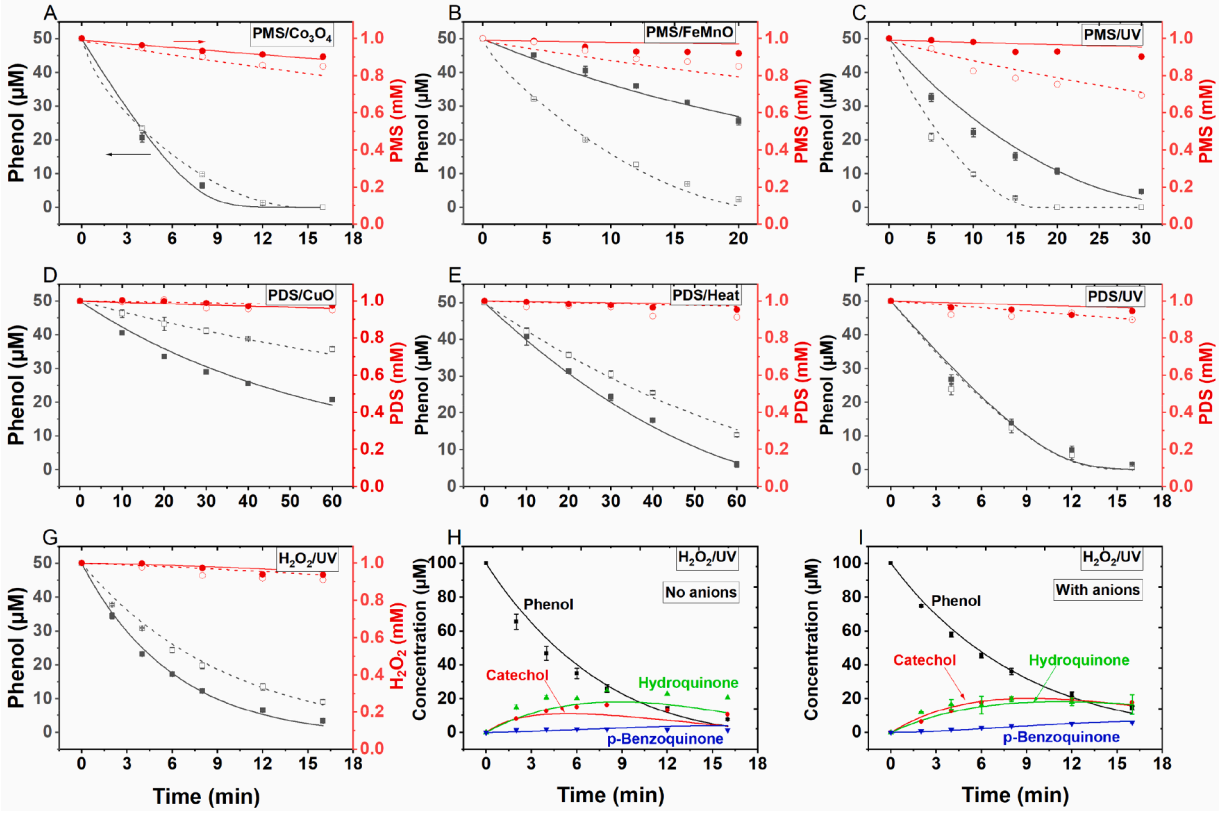

Fig. 2. (**A-G**) Stage 2 model improvement by fitting against the experimental phenol degradation (black) and oxidant consumption (red) data of the systems PMS/Co_3O_4, PMS/FeMnO, PMS/UV, PDS/CuO, PDS/heat, PDS/UV, and H_2O_2/UV, with or without the anions. The solid and open symbols are the experimental data in the absence and presence of the anions, respectively. The solid and dashed lines are the model simulation results. Experimental conditions: $[oxidant]_0 = 1$ mM, $[phenol]_0 = 50$ μM, pH = 7 with 20 mM borate buffer, and 70 °C for PDS/heat systems. (**H-I**) Model tuning by fitting against the experimental data of the systems H_2O_2/UV with and without the anions under the conditions: $[H_2O_2]_0 = 2$ mM, $[phenol]_0 = 100$ μM, pH = 7 with 20 mM borate buffer. "With anions" indicated $[Cl^-]_0 = 141$ mM, $[Br^-]_0 = 0.05$ mM, and $[HCO_3^-]_0 = 11.5$ mM. Error bars represent the data ranges of experimental replicates ($n \geq 2$).

model-fitted rate constant of PDS activation by heat was $7.8 \times 10^{-6}\, s^{-1}$, close to the reported value of $5.4 \times 10^{-6}\, s^{-1}$ under similar conditions (70 °C, pH 5) (Yang et al., 2019).

3.4. Model tuning (stage 3)

3.4.1. Inclusion of degradation intermediates

Although the model developed in stage 2 showed satisfactory fitting results for both phenol and the oxidants, the formation and further transformation of intermediates/products were still not included.

Overall, the oxidation of phenol by radical and non-radical species goes through two pathways, as illustrated in Schemes 1 A and B, respectively. More details can be found in Text S12 and Scheme S2.

After incorporating the above pathways into the model, we conducted another series of experiments with a higher initial phenol concentration for the systems of PMS/Co_3O_4, PDS/UV, and H_2O_2/UV, with or without the anions. Note that although not all the 7 systems were evaluated this time, the selected ones still covered all the three oxidants and two major activation approaches. As it is challenging to model all possible intermediates in AOPs even for simple compounds (Kamath et al., 2018), we initially only monitored some of the most important ones—catechol, hydroquinone, and p-benzoquinone. The model was then fit against the experimental data. As shown in Figs. 2H-I and S4, by treating four additional unknown rate constants (Reactions 279, 368, 369, and 483 in Table S2) as the fitting parameters, we observed good fittings for most of the monitored systems (R^2 = 0.72–0.99). This suggested that this comprehensive model can simulate the product transformation well. The details of the final model containing a total of 543 reactions can be found in Table S2.

3.4.2. Detailed balancing using DETBAL

The first round of detailed balancing analysis identified a total of 315 loops and two of them were illegal. The fundamental elements of these loops were reactions. The second round of analysis was performed by checking whether these small loops can form larger loops. As a result, a total of 24 illegal loops were further identified, each containing small loops as the elements. In addition, a total of 16 loops were found to disagree with the Wegscheider's condition (Fig. S2). These issues were fixed following the approaches described in Text S7. Because such a detailed balancing process has not been widely adopted in the literature, it would be helpful to keep but mark the reactions that were removed to illustrate the modifications, as shown in Table S2 (26 crossed and highlighted reactions). Overall, the removal of these reactions did not lead to significant changes in the concentrations of the species we monitored during the simulation, especially when no anions were present (data not shown).

3.5. Model validation (stage 4)

After the development of the model, a third batch of experiments was carried out for four systems, that is, PMS/UV and PDS/heat with and without the anions, to validate the model. As shown in Figs. 3A-C and S5A-B, the model demonstrated very good simulation for phenol and the intermediates in all the four systems (R^2 = 0.68–0.99). The differences in the intermediate formation in the PMS/UV systems without (Fig. 3A) and with (Figs. 3B and S5A) the anions were mainly due to the significant alteration of the major ROSs responsible for the phenol oxidation (Tables S9 and S10), which resulted in different pathways of intermediate formation (Scheme 1). The effects of the anions are further discussed in Section 3.6.

In addition to the experimental data collected in this study, the kinetic results for a few external systems were extracted from the literature for model validation. For example, an H_2O_2/UV system was selected under the experimental conditions of $[phenol]_0$ = 5.17 mM, $[H_2O_2]_0$ = 0.245 M, and temperature = 45 °C (Alnaizy and Akgerman, 2000). The UV irradiation parameters were slightly adjusted to reflect the different

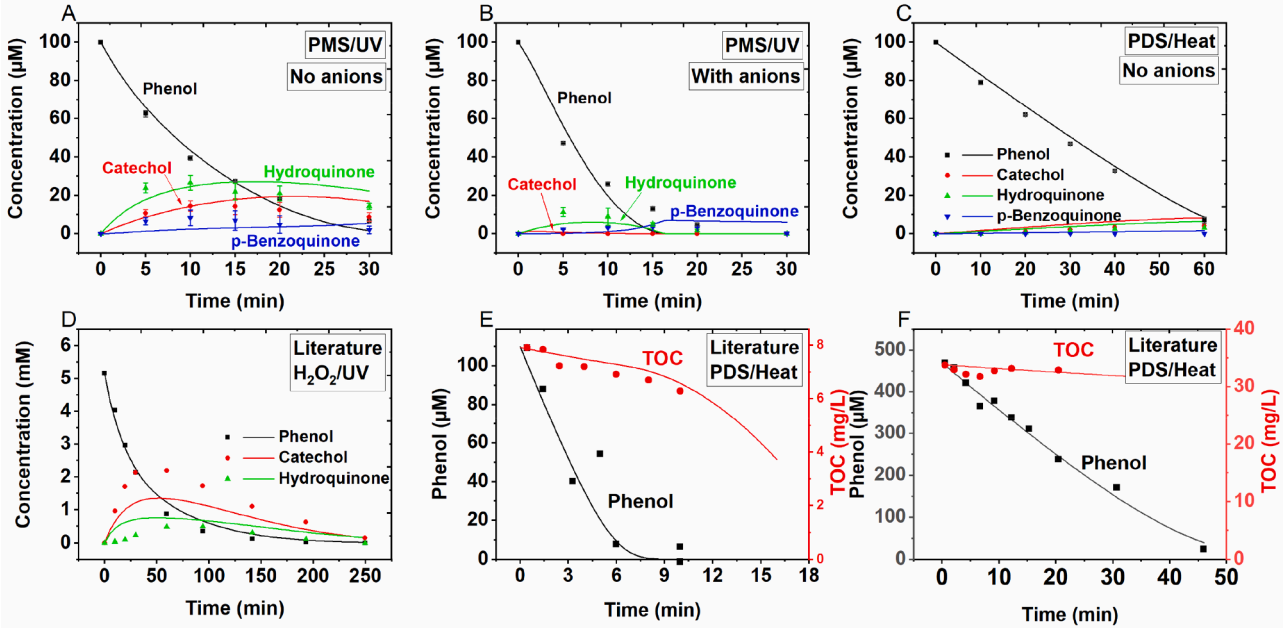

Fig. 3. First row: Model validation by fitting against the experimental data of systems (A) PMS/UV without the anions and (B) PMS/UV with the anions, both under the conditions: $[PMS]_0$ = 2 mM, $[phenol]_0$ = 100 μM, pH = 7 with 20 mM borate buffer; and (C) PDS/heat without the anions under conditions: $[PDS]_0$ = 2 mM, $[phenol]_0$ = 100 μM, pH = 7 with 20 mM borate buffer, and 70 °C. Error bars represent the data ranges of experimental replicates ($n \geq 2$). The transformation of two additional intermediates—o-chlorophenol and p-chlorophenol—in the PMS/UV system with anions can be found in Fig. S5A (it was too crowded to include them in Fig. 3B). Overall, the time courses of these two species were also very well simulated by the model, with the R^2 values of 0.99 and 0.92, respectively. Second row: Model validation by fitting against the data from the literature of systems (D) H_2O_2/UV under conditions: $[phenol]_0$ = 5.17 mM, $[H_2O_2]_0$ = 0.245 M, and 45 °C (Alnaizy and Akgerman, 2000); (E) PDS/heat under conditions: $[PDS]_0$ = 10 mM, $[phenol]_0$ = 110 μM, $[TOC]_0$ = 7.4 mg/L, pH = 2, and 70 °C (Mora et al., 2011); and (F) PDS/heat under conditions: $[PDS]_0$ = 10 mM, $[phenol]_0$ = 470 μM, $[TOC]_0$ = 31.8 mg/L, pH = 2, and 70 °C (Mora et al., 2011). "With anions" indicated $[Cl^-]_0$ = 141 mM, $[Br^-]_0$ = 0.05 mM, and $[HCO_3^-]_0$ = 11.5 mM.

UV intensity, effective path length and possible UV length. As shown in Fig. 3D, the model fitted moderately well to the degradation of phenol and the evolution of catechol and hydroquinone. We believe these fits are reasonable given that some of the reaction conditions were unknown, such as the ionic strength and potential introduction of halides during the solution preparation. Based on the kinetic data extrated from another study (Mora et al., 2011), the phenol and TOC (total organic carbon) removal was modeled for a PDS/heat system under three conditions, as shown in Figs. 3E-F and S5C. The TOC was calculated by the sum of the carbon weights from the major organic compounds, including phenol, o-, p-benzoquinones, and dihydroxybenzenes. Other species such as dihydroxybiphenyls and phenoxyphenols were also included but they did not make noticeable contributions (see the Excel file "Huang and Zhang_Kinetic modeling.xlsx" in the Supplementary Material for details). Surprisingly, the model demonstrated good fits (R^2 = 0.41–0.99) to the phenol and TOC trends although TOC was never used during the model development. In addition, we performed model fitting on a PDS/ZVI (zero-valent iron) system for p-chlorophenol oxidation (Zhao et al., 2010), a system which was not considered in our model. Because the mechanism is well known (that is, each PDS forms one sulfate radical upon activation, similar to the PMS/Co_3O_4 system), it is easy to simulate the system using our model. As shown in Fig. S5D, the fittings are also acceptable (R^2 = 0.63–0.82), given many uncertainties such as certain unknown interactions between ZVI and PDS, unknown starting pH (but likely near neutral), unknown ionic strength, and some potential co-existing ions that were not reported in the study. This further validated the obtained model.

3.6. Effects of the anions and contributions of different ROSs

With the developed model, the phenol degradation kinetics and the contribution of different ROSs can be easily simulated under different reaction conditions. We added different combinations of Cl^-, Br^-, and HCO_3^- to examine how the systems responded to the additions. As shown in Tables S9 and S10, in the absence of the anions, the phenol degradation in all the systems is almost always attributed to well-known ROSs or pathways—this result was obtained by simply tracking the phenol reactions with all the reactive species in the Kintecus program (details in Text S13). For example, in Table S9, $SO_4^{\bullet-}$ contributed to 99.8% of the phenol degradation in the PMS/Co_3O_4 system, and direct electron transfer was responsible for 100% in the PMS/FeMnO system. However, in the presence of the three anions, the largest contributors in the PMS/Co_3O_4 system shifted to $CO_3^{\bullet-}$ (72.2%) and HOBr (11.5%), while $SO_4^{\bullet-}$ only contributed 4.6%. A similar phenomenon existed in all other PMS systems. In addition to the reactions of the anions with the radicals, Cl^- and Br^- can also react with PMS at relatively high rates (k = 1.8×10^{-3} and 0.7 $M^{-1} s^{-1}$, respectively) to form HOX and subsequently other non-radical RHSs (Huang and Zhang, 2020b). These intermediates (non-radical RHSs) could be abundant and contributed to the fast phenol oxidation. Therefore, the PMS systems can be susceptible to the matrix effects. For the PDS systems in the absence of the anions (Table S10), direct electron transfer, $SO_4^{\bullet-}$, and $SO_4^{\bullet-}$ contributed to around 100% of phenol degradation in the PDS/CuO, PDS/Heat, and PDS/UV systems, respectively. In the presence of the three anions, however, the key species were found to be $S_2O_8^{\bullet-}$ in both the PDS/Heat and PDS/UV systems. None of the three anions affected the PDS/CuO system. As mentioned earlier, the PDS/CuO system under neutral conditions solely relies on direct electron transfer for phenol oxidation. Therefore, no new ROSs were generated to a noticeable level to alter the reaction mechanism.

For the H_2O_2/UV system, $^{\bullet}OH$ contributed to more than 80% of the phenol degradation under all the conditions. This indicates that H_2O_2/UV has high robustness after PDS/CuO, followed by all other systems. This agrees well with a study reporting that Cl^- did not exhibit noticeable effects on the 2,4,6-trichlorophenol oxidation and product formation in an H_2O_2/UV system (Fang et al., 2016). This might be due to the milder scavenging effects of the anions on $^{\bullet}OH$ than on $SO_4^{\bullet-}$. As shown in Eqs. A and B, X^- generally reacts with $^{\bullet}OH$ to form $HOX^{\bullet-}$, which proceeds to form OH^- and $X^{\bullet}$. In contrast, X^- often reacts with $SO_4^{\bullet-}$ to directly form SO_4^{2-} and $X^{\bullet}$. According to the rate constants of Reactions 37–42, 62–64, 66, and 67 (Table S2), such a scavenging effect is much more pronounced on $SO_4^{\bullet-}$ than on $^{\bullet}OH$. This has also been reported in another study (Zhang and Parker, 2018). Therefore, following the PDS/CuO system, H_2O_2/UV would be the second most robust system regarding the effect of halides.

$$^{\bullet}OH + X^- \rightleftharpoons HOX^{\bullet-} \rightleftharpoons OH^- + X^{\bullet} \quad (A)$$

$$SO_4^{\bullet-} + X^- \rightleftharpoons SO_4^{2-} + X^{\bullet} \quad (B)$$

In addition, we examined the effects of anion concentrations on the ROS contribution to phenol degradation. As shown in Fig. 4, upon the addition of the initial amounts of the anions, the dominant ROS in all the six systems shifted significantly from the original ones (e.g., $SO_4^{\bullet-}$ and/or $^{\bullet}OH$) to anion-related analogues (e.g., $Cl_2^{\bullet-}$, $CO_3^{\bullet-}$, HOBr, HOCl). With the further increase in the anion concentrations, some ROSs showed increased and then decreased contributions, while the rest demonstrated continuously increasing importance. The detailed shifting patterns are highly system-dependent. However, in the PDS/CuO system where phenol was always degraded through the direct electron transfer pathway, the presence of the anions did not affect the ROS contribution regardless of the anion concentrations (data not shown).

The major reason that we did not consider additional anions such as phosphate and nitrate is that they generally have much less impact on the AOP systems investigated in this study. As shown in Table S11, the second order reaction rate constants of these anions with sulfate and hydroxyl radicals are 2–6 orders of magnitude lower that those with the selected three anions. The presence of NOM was not considered either, mainly due to its lower reaction rates with radicals in radical-based systems (Lee et al., 2020a). In non-radical systems, NOM is often less competitive compared to target pollutants due to its low electron richness while non-radical systems are very selective toward electron-rich species (i.e., the target substrate) (Duan et al., 2018b; Lee et al., 2020a). In addition, there are many different types of NOMs, including different humic acids, fulvic acids, and humins. It can be very challenging to examine all representative NOMs for this modeling study. Furthermore, studies have reported that the effects of NOM are much more complex than just scavenging ROS which can occur in both the aqueous phase and the catalyst surface. NOM may also shade the photocatalytic materials from incoming photons or adsorb to the photocatalyst surfaces to potentially interfere with ROS production (Brame et al., 2015). The effects of different types of NOM may also vary significantly. Considering such challenges and complexities, we believe it is beyond the scope of this study to investigate the effects of NOM in this work.

3.7. Prediction of intermediate formation

Another advantage of having a comprehensive model is to easily predict the intermediate formation under different conditions without having to carry out any experiments. The simulated product formation for different systems and conditions are shown in Tables S12 and S13. HCO_3^- slightly altered the product distribution but did not change the types of products for all the systems. Upon the addition of Cl^- and/or Br^-, however, significant amounts of halogenated products such as halophenols, dihalophenols, and haloresorcinols formed in all the PMS-based systems. As mentioned above, this shift was primarily due to the formed non-radical RHSs resulting in the halide-substitution reactions. In contrast, halides did not exhibit such an effect in any of the PDS or H_2O_2 systems because of the negligible formation of non-radical RHSs. Further, although halides can result in radical RHSs in some of the systems, as mentioned above, these RHSs generally oxidize organic compounds through electron transfer reactions rather than halide

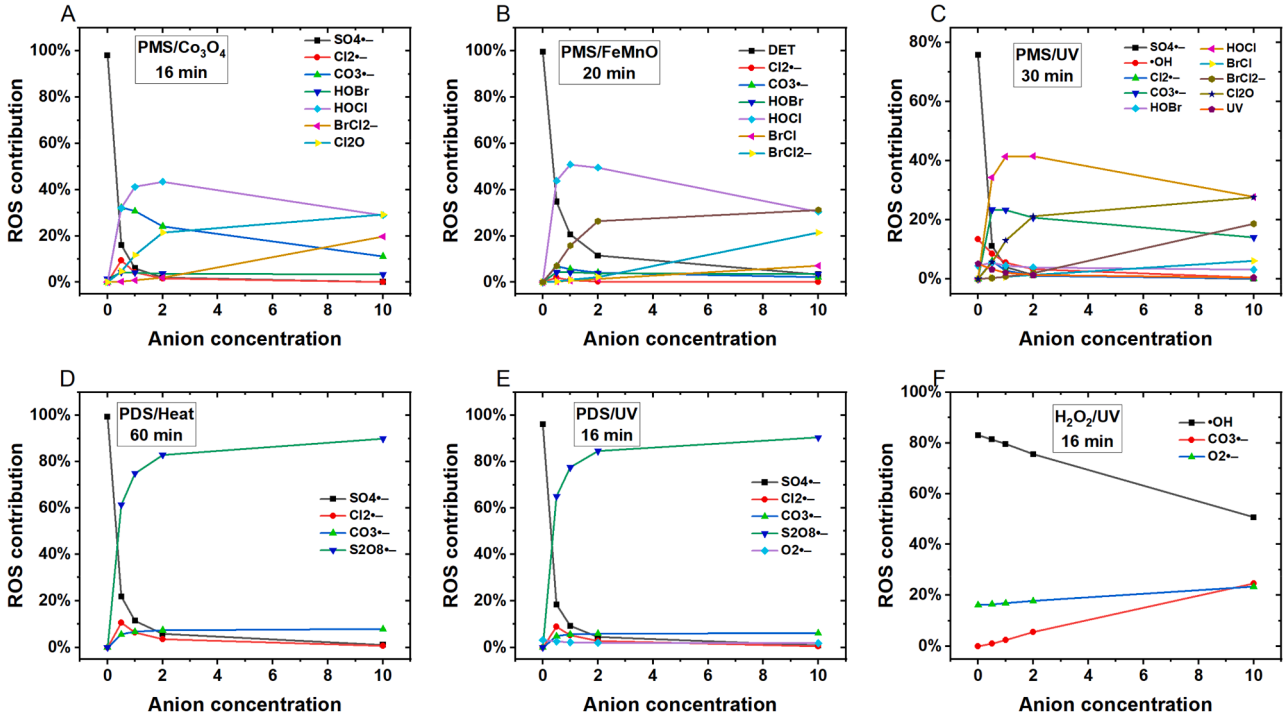

Fig. 4. Model simulated percentages of phenol oxidized by different ROSs at the given reaction times for the following systems: (A) PMS/Co_3O_4, (B) PMS/FeMnO, (C) PMS/UV, (D) PDS/Heat, (E) PDS/UV, and (F) H_2O_2/UV. Conditions: $[oxidant]_0$ = 1 mM, $[phenol]_0$ = 50 μM, pH = 7 with 20 mM borate buffer. The baseline anion concentrations are $[Cl^-]_0$ = 141 mM, $[Br^-]_0$ = 0.05 mM, and $[HCO_3^-]_0$ = 11.5 mM. Their concentrations on the X axis are a factor of 0-10 of the baseline concentration. For example, "10″ means the concentrations are 10 times of the baseline level.

substitution (Grebel et al., 2010). This agrees well with another study reporting that only 0.03% of halophenols formed in an H_2O_2/UV system with a halide level similar to that in this study (Grebel et al., 2010). Therefore, we conclude that the formation of halogenated byproducts would primarily be a concern for the PMS-based systems but not for the PDS or H_2O_2 systems, especially when the halide concentrations are low and the reaction time is short (e.g., less than 60 min). Although not modeled, the system of PMS/base may not form halogenated byproducts either because the reactions between PMS and halides can be significantly retarded under alkaline conditions (Huang and Zhang, 2020b).

3.8. Model sensitivity analysis

To understand the reaction importance, we performed sensitivity analysis for all the systems in the presence of anions by including all the initiation reactions in Table S5. In other words, all the seven systems were included in one model. Because any changes in the system setup, experimental conditions, or reaction time (as mentioned below) can potentially change the ranking of the reactions, this section mainly focuses on a qualitative demonstration rather than quantitative evaluation of the reaction importance. One can use this model to perform similar sensitivity analysis for a given scenario, and analyze the results with Atropos in Kintecus depending on their needs (Lee et al., 2020b). As shown in the Excel file "Huang and Zhang_Kinetic modeling.xlsx" in the Supplementary Material and Fig. S6, the model simulation-based sensitivity analysis was conducted for the beginning (1 s), the middle (480 s), and the end (960 s) of the reactions. However, as some of the reactions have not started at the beginning while others have already completed at the end, the sensitivity analyses for the systems at these times may not accurately reflect the real importance of these reactions. Therefore, hereafter we mainly interpret the results at the middle of the simulated reactions (480 s). Positive NSCs indicate positive contributions of the corresponding reactions to the corresponding species while negative results suggest negative contributions. Larger absolute NSC values generally mean higher importance of the reactions. As different reactions contribute differently to different species, and the species of interest usually change from one case to another, we decided to sum all the positive, negative, and absolute NSC values for each reaction to show their overall importance to the whole system, as shown in the sheet "Sensitivity_480 s, columns 'DP, DQ, and DR'" in the Excel file.

A total of 26 reactions (highlighted) were found to have no or minimum contributions to all the species. Most of these reactions involve uncommon species such as BrO_2^-, $BrOCl{\bullet}H_2O$, and $BrClO_2$. The reason that these reactions are not important might be related to the specific simulation conditions applied. Under other conditions, they might be important. On the other hand, it is interesting to know that overall, Reaction 144 ($CO_3^{\bullet-} + H_2O_2 \rightarrow HCO_3^- + HO_2^{\bullet}$) was the most important (but negatively). Reaction 149 ($CO_3^{\bullet-} + S_2O_8^{2-} \rightarrow CO_3^{2-} + S_2O_8^{\bullet-}$) had the largest positive contribution followed by Reaction 165 ($Br^- + HSO_5^- \rightarrow HOBr + SO_4^{2-}$). This might be because the formed $S_2O_8^{\bullet-}$ and HOBr are strong oxidants and can oxidize a wide range of organics or facilitate other reactions. More details about the importance of each reaction can be found in the Excel file. By using the filters in the spreadsheet, one can check which reaction is the most important for a specific species. Overall, all the top reactions are those we are already familiar with, and many of them have been included in Scheme S1. It is also interesting to know that many reactions (especially those related to the anions) are more important than the initiation reactions in Table S5. This explains why the presence of anions in some cases significantly altered the reaction pathways and the product formation. With this sensitivity analysis approach, one can also easily understand why and how different reaction conditions affect the target system.

3.9. Model applicability to other reaction systems or contaminants

Although the development of this model only involved seven systems, it covers most of the known reaction mechanisms in AOPs using PMS, PDS, or H_2O_2 as the oxidant, including radical, non-radical, and

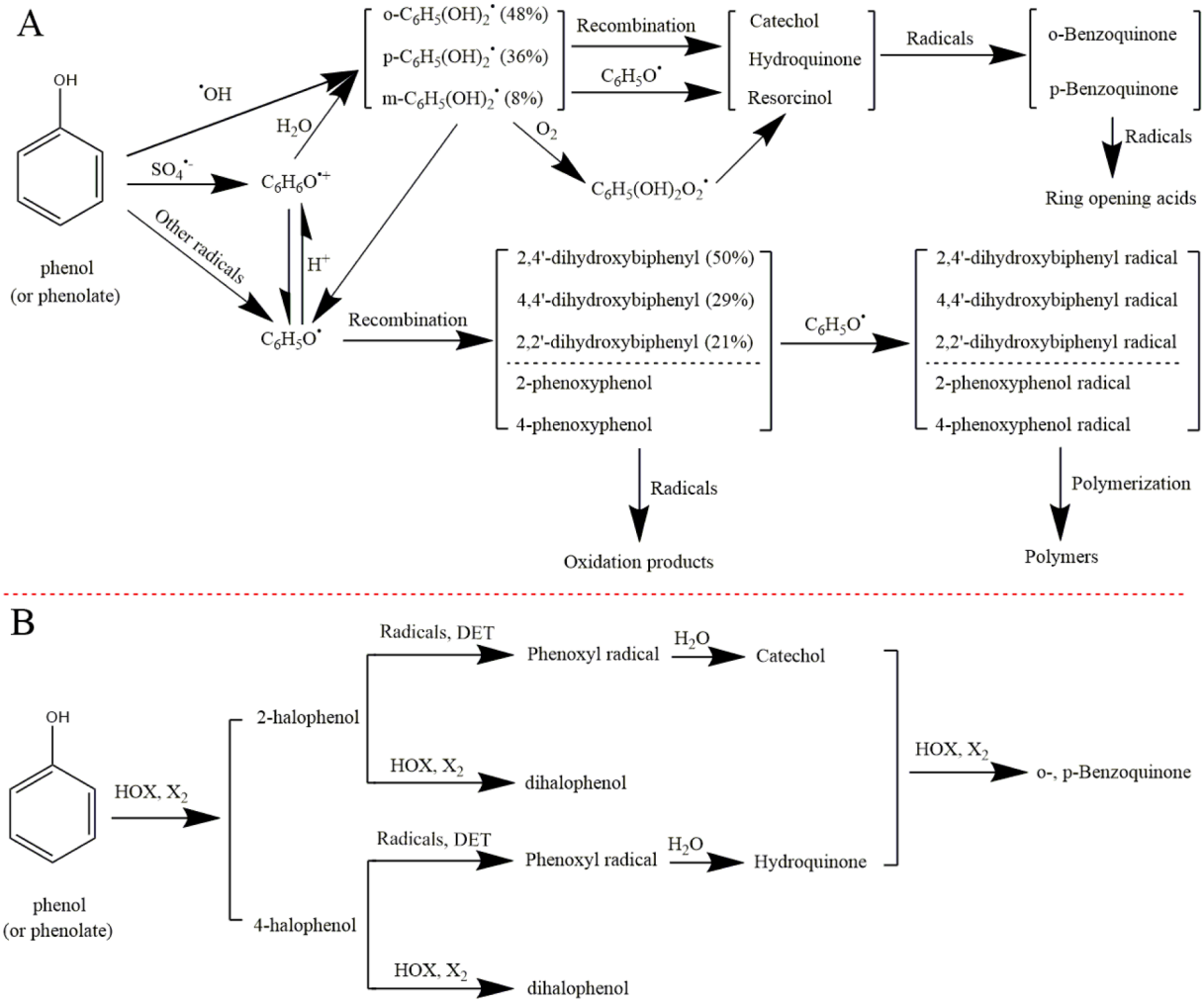

Scheme 1. Pathways of phenol transformation by (A) radical ROSs and (B) non-radical RHSs.

direct electron transfer processes. Therefore, this model can be easily applied to many other systems (e.g., hybrid systems) with only minor modifications, mostly by adding necessary initiation reactions. For example, in a study where PDS and H_2O_2 were activated simultaneously by UV, catalyst, and heat (Monteagudo et al., 2015), existing models would not be able to provide mechanistic insights for the system. However, the model developed in this study can easily do so. For other AOPs pertaining to different oxidants such as ozone (e.g., O_3, O_3/UV, O_3/H_2O_2, and O_3/PMS), these systems generally form $^{\bullet}OH$ and/or $SO_4^{\bullet-}$ as the primary ROSs and, thus, can be well simulated using the current model as well.

This new model is also significant in that, although only phenol was used as the parent compound, it can be easily extended to many other contaminants. This is because nearly half of the reactions are about the ROS transformation and can be directly reused. In addition, phenol is the most basic phenolic compounds and shares significant similarity with many other contaminants. The transformation pathways of phenol can therefore be largely applied to other phenolic compounds in future models. As many phenol transformation intermediates, such as monohalophenols, dihalophenols, dihydroxybenzenes, and benzoquinones, were involved in this model, other AOP systems involving any of these species—either as parent compound or intermediate—can also adopt many of these reactions. Moreover, recent studies developed a computer program based on known reaction rules to automatically generate the reaction pathways for a given organic contaminant toward $^{\bullet}OH$ (Guo et al., 2014a, 2014b). The reaction rate constants of the intermediates/products with $^{\bullet}OH$ can also be predicted using reported QSAR models, which are under rapid development for different ROSs thanks to the application of machine learning (Zhong et al., 2020a, 2021, 2020b). The limitation of the computer program is that it is still limited to $^{\bullet}OH$. If it can be further improved to generate reaction pathways for other ROSs, it can be coupled with QSAR models and the model developed in this study to substantially expand the modeling applicability of these three tools.

In addition, compared to most of the models in the literature, the model developed in this study has provided both valuable methodologies and reusable contents with high quality for future model development.

4. Conclusion

This study first evaluated the performance (phenol degradation rates and oxidant utilization efficiencies) of four PMS, four PDS, and one H_2O_2 systems for phenol oxidation in the absence or presence of halides and carbonate. A comprehensive kinetic model was then built based on seven systems with over 540 reactions. Compared to previous modeling studies, this work considerably improved the model by combining all the major reactions and revising the reactions that have been inaccurately applied in other models. The observed transformation of a few intermediates/products provided a more detailed understanding of the systems. The application of various modeling approaches, from detailed balancing using DETBAL and overparameterization control to model

validation with additional measurements and external systems, also significantly improved the reliability of the obtained model. Different from most other kinetic models, which were built for mostly single systems, the model developed in this study can be applied to complex hybrid systems involving different oxidants and/or activation mechanisms. Our modeling results revealed that, among the seven AOPs, the PDS/CuO system was the most robust against the impact of halides and carbonate, followed by the H_2O_2/UV system, and then the other systems.

We observed that different AOP systems usually share many reactions, especially those associated with ROS. Therefore, developing a comprehensive model that can describe more than seven AOP systems does not necessarily require many more reactions. The development of this model was not simply a reaction-gathering process, but rather a systematic information integration process. For the first time, the dynamic radical formation rates for PMS, PDS, H_2O_2, HOBr, and HOCl under UV irradiation were employed considering the dynamic effects of co-existing species which can either block or absorb UV to reduce the intensity of UV available for radical formation.

Studies have suggested that more attention should be paid to the important reactions, and adding additional ones may not be able to improve the prediction accuracy (Bulman et al., 2019). This is true and easy for simple systems and when the target species are the major ones. However, for complex systems (e.g., hybrid systems) that involve multiple oxidants, activation approaches, and reaction mechanisms, it is usually hard to identify the most important reactions without having to compile many others. In addition, the importance of a reaction is always relative and subjective depending on the species of interest or the scope of the study. For example, the reactions that are important for mineralization of phenol are not necessarily important for its polymerization, whereas both pathways are of great research interest. It is tedious to develop new models each time for new goals even if they are for the same system. A comprehensive model can therefore be beneficial to avoid this by capturing all these pathways in one model and help identify the important reactions for specific scopes. It is then the user's decision about whether to use all or only the important ones.

However, this model still has a few limitations. First, the number of the experimentally measured intermediates is small, so the prediction of other intermediates may not be as reliable. Second, only three co-existing ions are considered in this study. In reality, many other ions and organics (e.g., NOM) may also be present in the target water. Their roles in the kinetic model and effects on the water treatment should be investigated as well. Third, the further transformation of some later-stage species such as the ring opening acids and polymers are not well captured yet, which requires additional work if they are of interest.

Declaration of Competing Interest

The authors declare that they have no known competing financial interests or personal relationships that could have appeared to influence the work reported in this paper.

Acknowledgments

This work was funded by the National Science Foundation Grant CHE-1808406.

Supplementary materials

Supplementary material associated with this article can be found, in the online version, at doi:10.1016/j.wroa.2021.100129.

References

Alfassi, Z.B., Huie, R.E., Mosseri, S., Neta, P., 1988. Kinetics of one-electron oxidation by the ClO radical. Radiat. Phys. Chem. 32 (1), 85–88.
Alnaizy, R., Akgerman, A., 2000. Advanced oxidation of phenolic compounds. Adv. Environ. Res. 4 (3), 233–244.
Brame, J., Long, M., Li, Q., Alvarez, P., 2015. Inhibitory effect of natural organic matter or other background constituents on photocatalytic advanced oxidation processes: mechanistic model development and validation. Water Res 84, 362–371.
Bulman, D.M., Mezyk, S.P., Remucal, C.K, 2019. The impact of pH and irradiation wavelength on the production of reactive oxidants during chlorine photolysis. Environ. Sci. Technol. 53 (8), 4450–4459.
Cheng, S., Zhang, X., Yang, X., Shang, C., Song, W., Fang, J., Pan, Y., 2018. The multiple role of bromide ion in PPCPs degradation under UV/Chlorine treatment. Environ. Sci. Technol. 52 (4), 1806–1816.
Chuang, Y.H., Chen, S., Chinn, C.J., Mitch, W.A, 2017. Comparing the UV/Monochloramine and UV/Free chlorine advanced oxidation processes (AOPs) to the UV/Hydrogen peroxide AOP under scenarios relevant to potable reuse. Environ. Sci. Technol. 51 (23), 13859–13868.
Crittenden, J.C., Hu, S., Hand, D.W., Green, S.A, 1999. A kinetic model for H2O2/UV process in a completely mixed batch reactor. Water Res 33 (10), 2315–2328.
Duan, X., Sanan, T., de la Cruz, A., He, X., Kong, M., Dionysiou, D.D, 2018a. Susceptibility of the algal toxin microcystin-LR to UV/chlorine process: comparison with chlorination. Environ. Sci. Technol. 52 (15), 8252–8262.
Duan, X., Sun, H., Shao, Z., Wang, S., 2018b. Nonradical reactions in environmental remediation processes: uncertainty and challenges. Appl. Catal. B-Environ. 224, 973–982.
Duesterberg, C.K., Waite, T.D, 2006. Process optimization of Fenton oxidation using kinetic modeling. Environ. Sci. Technol. 40 (13), 4189–4195.
Duesterberg, C.K., Waite, T.D, 2007. Kinetic modeling of the oxidation of p-hydroxybenzoic acid by Fenton's reagent: Implications of the role of quinones in the redox cycling of iron. Environ. Sci. Technol. 41 (11), 4103–4110.
Fang, C., Xiao, D., Liu, W., Lou, X., Zhou, J., Wang, Z., Liu, J., 2016. Enhanced AOX accumulation and aquatic toxicity during 2,4,6-trichlorophenol degradation in a Co (II)/peroxymonosulfate/Cl(-) system. Chemosphere 144, 2415–2420.
Grebel, J.E., Pignatello, J.J., Mitch, W.A, 2010. Effect of halide ions and carbonates on organic contaminant degradation by hydroxyl radical-based Advanced Oxidation Processes in saline waters. Environ. Sci. Technol. 44 (17), 6822–6828.
Guo, X., Minakata, D., Crittenden, J., 2014a. Computer-based first-principles kinetic Monte Carlo simulation of polyethylene glycol degradation in aqueous phase UV/H2O2 advanced oxidation process. Environ. Sci. Technol. 48 (18), 10813–10820.
Guo, X., Minakata, D., Niu, J., Crittenden, J., 2014b. Computer-based first-principles kinetic modeling of degradation pathways and byproduct fates in aqueous-phase advanced oxidation processes. Environ. Sci. Technol. 48 (10), 5718–5725.
Held, A.M., Halko, D.J., Hurst, J.K, 1978. Mechanisms of chlorine oxidation of hydrogen peroxide. J. Am. Chem. Soc. 100 (18), 5732–5740.
Huang, K.Z., Zhang, H., 2019. Direct electron-transfer-based peroxymonosulfate activation by iron-doped manganese oxide (δ-MnO2) and the development of Galvanic Oxidation Processes (GOPs). Environ. Sci. Technol. 53 (21), 12610–12620.
Huang, K.Z., Zhang, H., 2020a. Galvanic oxidation processes (GOPs): an effective direct electron transfer approach for organic contaminant oxidation. Sci. Total Environ. 743, 140828.
Huang, K.Z., Zhang, H., 2020b. Highly efficient bromide removal from shale gas produced water by unactivated peroxymonosulfate for controlling disinfection byproduct formation in impacted water supplies. Environ. Sci. Technol. 54 (8), 5186–5196.
Ianni, J.C. Kintecus, Windows version 6.8, 2019. www.kintecus.com.
Kamath, D., Mezyk, S.P., Minakata, D., 2018. Elucidating the elementary reaction pathways and kinetics of hydroxyl radical-induced acetone degradation in aqueous phase advanced oxidation processes. Environ. Sci. Technol. 52 (14), 7763–7774.
Kang, N., Lee, D.S., Yoon, J., 2002. Kinetic modeling of Fenton oxidation of phenol and monochlorophenols. Chemosphere 47 (9), 915–924.
Khan, A.U., Kasha, M., 1970. Chemiluminescence arising from simultaneous transitions in pairs of singlet oxygen molecules. J. Am. Chem. Soc. 92 (11), 3293–3300.
Kong, X., Wu, Z., Ren, Z., Guo, K., Hou, S., Hua, Z., Li, X., Fang, J., 2018. Degradation of lipid regulators by the UV/chlorine process: radical mechanisms, chlorine oxide radical (ClO(*))-mediated transformation pathways and toxicity changes. Water Res 137, 242–250.
Lee, J., von Gunten, U., Kim, J.H., 2020a. Persulfate-based advanced oxidation: critical assessment of opportunities and roadblocks. Environ. Sci. Technol. 54 (6), 3064–3081.
Lee, W., Lee, Y., Allard, S., Ra, J., Han, S., Lee, Y., 2020b. Mechanistic and kinetic understanding of the UV254 photolysis of chlorine and bromine species in water and formation of oxyhalides. Environ. Sci. Technol. 54 (18), 11546–11555.
Li, K., Stefan, M.I., Crittenden, J.C, 2004. UV photolysis of trichloroethylene: product study and kinetic modeling. Environ. Sci. Technol. 38 (24), 6685–6693.
Li, K., Stefan, M.I., Crittenden, J.C., 2007. Trichloroethene degradation by UV/H2O2 advanced oxidation process: product study and kinetic modeling. Environ. Sci. Technol. 41 (5), 1696–1703.
Li, X., Liu, J., Rykov, A.I., Han, H., Jin, C., Liu, X., Wang, J., 2015. Excellent photo-Fenton catalysts of Fe–Co Prussian blue analogues and their reaction mechanism study. Appl. Catal. B-Environ. 179, 196–205.
Lin, J.-.M., Liu, M., 2008. Chemiluminescence from the decomposition of peroxymonocarbonate catalyzed by gold nanoparticles. J. Phys. Chem. B 112 (26), 7850–7855.
Liu, M., Zhao, L., Lin, J.-.M, 2006. Chemiluminescence energy transfer reaction for the on-line preparation of peroxymonocarbonate and Eu(II)−dipicolinate complex. J. Phys. Chem. A 110 (23), 7509–7514.
Luo, C., Sadhasivan, M., Kim, J., Sharma, V.K., Huang, C.H, 2021. Revelation of Fe(V)/Fe(IV) Involvement in the Fe(VI)-ABTS System: kinetic Modeling and Product Analysis. Environ. Sci. Technol. 55 (6), 3976–3987.

Luo, R., Li, M., Wang, C., Zhang, M., Nasir Khan, M.A., Sun, X., Shen, J., Han, W., Wang, L., Li, J., 2019. Singlet oxygen-dominated non-radical oxidation process for efficient degradation of bisphenol A under high salinity condition. Water Res 148, 416–424.

Monteagudo, J.M., Durán, A., González, R., Expósito, A.J., 2015. In situ chemical oxidation of carbamazepine solutions using persulfate simultaneously activated by heat energy, UV light, Fe2+ ions, and H2O2. Appl. Catal. B-Environ. 176-177, 120–129.

Mora, V.C., Rosso, J.A., Martire, D.O., Gonzalez, M.C, 2011. Phenol depletion by thermally activated peroxydisulfate at 70 °C. Chemosphere 84 (9), 1270–1275.

Olmez-Hanci, T., Arslan-Alaton, I., 2013. Comparison of sulfate and hydroxyl radical based advanced oxidation of phenol. Chem. Eng. J. 224, 10–16.

Pavitt, A.S., Bylaska, E.J., Tratnyek, P.G, 2017. Oxidation potentials of phenols and anilines: correlation analysis of electrochemical and theoretical values. Environ. Sci.: Process. Impacts 19 (3), 339–349.

Piatt, J., O'brien, P.J., 1979. Singlet oxygen formation by a peroxidase, H2O2 and halide system. Eur. J. Biochem. 93 (2), 323–332.

Qi, C., Liu, X., Ma, J., Lin, C., Li, X., Zhang, H., 2016. Activation of peroxymonosulfate by base: implications for the degradation of organic pollutants. Chemosphere 151, 280–288.

Qian, Y., Guo, X., Zhang, Y., Peng, Y., Sun, P., Huang, C.H., Niu, J., Zhou, X., Crittenden, J.C, 2016. Perfluorooctanoic acid degradation using UV-persulfate process: modeling of the degradation and chlorate formation. Environ. Sci. Technol. 50 (2), 772–781.

Wang, J., Wang, S., 2018. Activation of persulfate (PS) and peroxymonosulfate (PMS) and application for the degradation of emerging contaminants. Chem. Eng. J. 334, 1502–1517.

Wang, Z., Feng, M., Fang, C., Huang, Y., Ai, L., Yang, F., Xue, Y., Liu, W., Liu, J., 2017. Both degradation and AOX accumulation are significantly enhanced in UV/peroxymonosulfate/4-chlorophenol/Cl− system: two sides of the same coin? RSC Adv. 7 (20), 12318–12321.

Wu, Z., Fang, J., Xiang, Y., Shang, C., Li, X., Meng, F., Yang, X., 2016. Roles of reactive chlorine species in trimethoprim degradation in the UV/chlorine process: kinetics and transformation pathways. Water Res 104, 272–282.

Yang, F., Sheng, B., Wang, Z., Yuan, R., Xue, Y., Wang, X., Liu, Q., Liu, J., 2019. An often-overestimated adverse effect of halides in heat/persulfate-based degradation of wastewater contaminants. Environ. Int. 130, 104918.

Yang, Y., Pignatello, J.J., Ma, J., Mitch, W.A, 2014. Comparison of halide impacts on the efficiency of contaminant degradation by sulfate and hydroxyl radical-based advanced oxidation processes (AOPs). Environ. Sci. Technol. 48 (4), 2344–2351.

Yang, Y., Pignatello, J.J., Ma, J., Mitch, W.A, 2016. Effect of matrix components on UV/H2O2 and UV/S2O8(2-) advanced oxidation processes for trace organic degradation in reverse osmosis brines from municipal wastewater reuse facilities. Water Res 89, 192–200.

Zagal, J.H., Ponce, I., Oñate, R., 2019. Redox Potentials as Reactivity Descriptors in Electrochemistry. In *Redox*. IntechOpen.

Zhang, K., Parker, K.M, 2018. Halogen radical oxidants in natural and engineered aquatic systems. Environ. Sci. Technol. 52 (17), 9579–9594.

Zhang, R., Sun, P., Boyer, T.H., Zhao, L., Huang, C.H, 2015. Degradation of pharmaceuticals and metabolite in synthetic human urine by UV, UV/H2O2, and UV/PDS. Environ. Sci. Technol. 49 (5), 3056–3066.

Zhao, J., Zhang, Y., Quan, X., Chen, S., 2010. Enhanced oxidation of 4-chlorophenol using sulfate radicals generated from zero-valent iron and peroxydisulfate at ambient temperature. Sep. Purif. Technol. 71 (3), 302–307.

Zhao, X., Li, Y., Lu, J., Zhou, L., Chovelon, J.-.M., Zhou, Q., Ji, Y., 2021. UV/H2O2 oxidation of chloronitrobenzenes in waters revisited: hydroxyl radical induced self-nitration. J. Photochem. Photobiol. A: Chem. 410, 113162.

Zhong, S., Hu, J., Fan, X., Yu, X., Zhang, H., 2020a. A deep neural network combined with molecular fingerprints (DNN-MF) to develop predictive models for hydroxyl radical rate constants of water contaminants. J. Hazard. Mater. 383, 121141.

Zhong, S., Hu, J., Yu, X., Zhang, H., 2021. Molecular image-convolutional neural network (CNN) assisted QSAR models for predicting contaminant reactivity toward OH radicals: transfer learning, data augmentation and model interpretation. Chem. Eng. J. 408, 127998.

Zhong, S., Zhang, K., Wang, D., Zhang, H., 2020b. Shedding Light On "Black Box" Machine Learning Models for Predicting the Reactivity of HO• Radicals toward Organic Compounds. Chem. Eng. J., 126627

Zhou, L., Song, W., Chen, Z., Yin, G., 2013. Degradation of organic pollutants in wastewater by bicarbonate-activated hydrogen peroxide with a supported cobalt catalyst. Environ. Sci. Technol. 47 (8), 3833–3839.

Zhou, Y., Jiang, J., Gao, Y., Pang, S.Y., Ma, J., Duan, J., Guo, Q., Li, J., Yang, Y., 2018. Oxidation of steroid estrogens by peroxymonosulfate (PMS) and effect of bromide and chloride ions: kinetics, products, and modeling. Water Res 138, 56–66.